The response of macrophages and their osteogenic potential modulated by micro/nano-structured Ti surfaces

Wentao Liu [a], Luxin Liang [a], Bo Liu [b, ***], Dapeng Zhao [c], Yingtao Tian [d], Qianli Huang [a, e, **], Wu Hong [a, *]

[a] State Key Laboratory of Powder Metallurgy, Central South University, Changsha 410083, P. R. China

[b] Department of General Surgery, The Second Xiangya Hospital, Central South University, Changsha 410011, P. R. China

[c] College of Biology, Hunan University, Changsha 410082, P. R. China

[d] Engineering Department, Lancaster University, Lancaster, UK

[e] Foshan (Southern China) Institute for New Materials, Foshan 528200, P. R. China

E-mail: hwucsu@csu.edu.cn (Hong Wu), hql1990@163.com (Qianli Huang), liubomri@csu.edu.cn (Bo Liu)

Abstract

Current understanding on the interactions between micro/nano-structured Ti surfaces and macrophages is still limited. In this work, TiO_2 nano-structures were introduced onto acid-etched Ti surfaces by alkali-heat treatment, ion exchange and subsequent heat treatment. By adjusting the concentration of NaOH during alkali-heat treatment, nano-flakes, nano-flakes mixed with nano-wires or nano-wires could formed on acid-etched Ti surfaces. The micro- and micro/nano-structured Ti surfaces possessed similar surface chemical and phase compositions. *In vitro* results indicate that the morphology of macrophages was highly dependent on the morphological features of nano-structures. Nano-flakes and nano-wires were favorable to induce the formation of lamellipodia and filopodia, respectively. Compared to micro-structured Ti surface, micro/nano-structured Ti surfaces polarized macrophages to their M2 phenotype and enhanced the gene expressions of osteogenic growth factors in macrophages. The M2 polarized macrophages promoted the maturation of osteoblasts. Compared to that with nano-flakes or nano-wires, the surface with mixed features of nano-flakes and nano-wires exhibited stronger anti-inflammatory and osteo-immunomodulatory effects. The findings presented in the current work suggest that introducing micro/nano-topographies onto Ti-based implant surfaces is a promising strategy to modulate the inflammatory response and mediate osteogenesis.

Keywords: Ti implant, surface modification, micro/nano-structured surface, macrophage polarization, osteoblast differentiation

1. Introduction

Titanium (Ti) and its alloys are extensively used in orthopedics and dentistry owing to their good mechanical properties, excellent biocompatibility and outstanding corrosion resistance [1]. The integration between Ti-based implants and bone tissue is generally achieved through a series of complex biological processes including coagulation, inflammation, bone healing and remodeling [2, 3]. In recent years, the development of osteoimmunology has gradually revealed the shared signaling biomolecules and crosstalk between the skeleton and immune system [4]. As an innate immune response, the inflammation induced by biomaterial implantation has been realized to significantly regulate subsequent bone healing and modeling [5, 6]. However, the inflammation-modulatory function of bone biomaterials did not receive sufficient attention in the past decades.

Among various kinds of immune cells, macrophages are widely accepted to be mainly responsible for biomaterial-induced inflammatory response. In general, macrophages can be classed into two subtypes including pro-inflammatory M1 phenotype and anti-inflammatory M2 phenotype [7, 8]. The former one is capable of secreting abundant pro-inflammatory cytokines such as tumor necrosis factor-α (TNF-α), interleukin-6 (IL-6) and IL-1β, while the latter one favors in the release of anti-inflammatory cytokines including IL-10 and arginase-1 (Arg-1) [9, 10]. Moreover, the macrophages are highly plastic so that they can flexibly switch their phenotypes and functions in response to various kinds of stimuli such as topographical clues, superficial chemical features, bio-functional ions and molecules [6, 11-13]. Therefore, it is of great importance to consider the regulatory effects of biomaterials on macrophage phenotypes and functions during material design and development.

Ti-based implants are commonly subjected to surface modification which targets at altering material surface chemistry and/or topography for enhanced bone regeneration [14, 15]. Among surface topographical design, micro/nano-structured surfaces have received extensive attention because they can interact with multi-scale biological components such as proteins and cells [16, 17]. There are *in vitro* and *in vivo* evidences showing that micro/nano-topographical surfaces could direct modulate the response of bone forming cells such as mesenchymal stem cells (MSCs), osteoblasts and osteoclasts [18-20]. However, the interactions between micro/nano-topographical clues on Ti surfaces and macrophages have been explored limitedly. We previously reported that the surface characteristics of micro-structured Ti surface decorated with bio-ceramics nano-particles exhibited anti-inflammatory effect on macrophage polarization [11]. Bai et al. found that micro/nano-structured Ti surface with hydroxyapatite nano-particles and nano-rods induced M2 and M1 polarization in macrophages, respectively

[21]. Li et al. reported that micro-arc oxidized micro/nano-structured Ti surfaces deposited with silver (Ag) nano-particles (~20 nm) activated both M1 and M2 phenotype in macrophages within 5 days, while polarized macrophages to their M2 extreme in the later stage (day 7) [22]. These works suggest that micro/nano-structured Ti surfaces could modulate the polarization behavior of macrophages, while they failed to decouple the influence of surface topography and chemistry on macrophage response. To elucidate the effect of micro/nano-topography on macrophage activation, it is of great importance to ensure that the micro- and nano-structures are highly similar in chemical and phase compositions. So far, previously reported suitable micro/nano-structured models for macrophage polarization investigation are mainly limited to TiO_2 nanotubes with different sizes grown on micro-topographical Ti substrates [23, 24]. Therefore, the modulatory roles of micro-structured Ti surfaces decorated with other TiO_2 nano-structures on macrophage polarization are worthy of investigation.

In this study, micro-structured Ti surfaces were prepared by acid etching. Subsequently, various nanostructures including nano-flakes, nano-wires and nano-flakes mixed with nano-wires were introduced onto micro-structured Ti surfaces *via* alkali-heat treatment, ion exchange and subsequent heat treatment. The modulatory roles of as-prepared micro/nano-structured Ti surfaces on macrophage polarization were investigated. In addition, the osteogenic capacities of the inflammatory micro-environments created by surface-macrophage interactions were explored.

2. Materials and methods

2.1 Preparation of micro/nano-structured Ti surfaces

Commercially pure Ti discs with a diameter of 13.5 mm and thickness of 2 mm were polished, cleaned and corroded twice (10 min each time) in an acid solution containing 2.5% HF, 12.5% HNO_3 (volume fraction) within an ultrasonic cleaning machine. After acid etching, the discs were rinsed twice in deionized water and dried in a vacuum drying chamber at 60 °C. As-treated specimens were noted as AE-Ti.

For alkali-heat treatment, each AE Ti disc was placed in a 100 mL Teflon-lined autoclave containing 60 mL NaOH solution. The treatment was conducted at 200 °C for 16 h in a furnace. Thereafter, the specimens were washed, immersed in 10% HCl solution (volume fraction) for 15 min for ion exchange and heated at 600 °C for 2 h. The concentration of NaOH solution employed for reaction was 0.5, 3 or 5 M. As-treated specimens were noted as AH0.5-, AH3- and AH5-Ti, respectively.

2.2 Physicochemical characterizations of the surfaces

The surface morphology was observed by dual-beam scanning electron microscopy (DBSEM; Helios Nanolab G3 UC, FEI, USA) equipped with energy dispersive X-ray spectroscopy (EDS). The surface roughness was measured using a confocal microscope (CM; LSM700, Olympus, Japan). The phase composition was detected by an X-ray diffractometer (XRD; Advance D8, Bruker, Germany). The surface chemistry was analyzed using X-ray photoelectron spectroscopy (XPS; ESCALAB250Xi, Thermo Fisher Scientific, USA). The surface wettability was measured by a contact angle meter (CAM; OCA 25LHT, Dataphysics instrument GmbH, Germany).

2.3 Cell culture and seeding

Human osteoblast-like SaOS-2 cells and murine-derived RAW 264.7 cells were selected as models for osteoblasts and macrophages, respectively. SaOS-2 cells were cultured in McCoy's complete medium consisted of 84% McCoy's medium (Gibco, USA), 15% fetal bovine serum (FBS; Gibco, USA) and 1% penicillin-streptomycin (PS; Gibco, USA). RAW 264.7 cells were incubated in HG-DMEM complete medium compose of 89% HG-DMEM (Gibco, USA), 10% FBS and 1% PS. Both kinds of cells were cultured in an incubator under a condition of 37 °C, 5% CO_2 and 95% humidity.

The specimens sterilized by an autoclave were placed in 24-well plates. The macrophages were seeded on each specimen surface at a density of 60, 000 cells per well. After culturing for 2 days, the medium in each group was collected, filtered by 0.22 μm filter membrane and then mixed with McCoy's complete medium at a volume ratio of 1:6. As-mixed medium was noted as macrophage-conditioned medium (MCM). SaOS-2 cells with a density of 15, 000 cells per well were directly seeded in each well of 24-well plates and incubated with various MCM.

2.4 Macrophage response to micro/nano-structured Ti surfaces

2.4.1 Cell proliferation

The proliferation of cells was quantified using cell-counting kit-8 (CCK-8; Dojindo, Japan) assay. At pre-defined time points, 270 μL HG-DMEM complete culture medium was mixed with 30 μL CCK-8 and added into each well for incubation for 30 min. Subsequently, 100 μL incubated solution from each well was transferred into a 96-well plate. The optical density (OD) values were measured by a multimode plate reader (Thermo Fisher Scientific, USA) at 450 nm. The viability of cells was evaluated by calcein-AM (Dojindo, Japan) staining. After culturing for 1 and 3 days, the cells were washed twice using phosphate buffered saline (PBS; Hyclone, USA). Subsequently, each specimen was incubated with 300 μL calcein-AM solution (2 μM in PBS) in darkness for 15 min at 37 °C and photographed using fluorescence microscopy (DSY-L140, Beijing Changheng Rongchuang Technology Co. LTD, China).

2.4.2 Cells morphology

After culturing for 2 days, the cells were fixed by 4% paraformaldehyde for 30 min, treated with 1% Triton X-100 solution for 5 min and incubated with 5 μL/mL phalloidin-fluorescein conjugate (Apexbio, USA) for 20 min at 37 °C. Thereafter, the cell nuclei were stained by 4′-6-diamidino-2-phenylindole (DPAI; Sigma, USA) for 30 s. The fluorescent images were recorded using a laser confocal microscope (LCM; FV1200, Olympus, Japan).

2.4.3 Gene expressions

On day 2, the cells were cracked by adding 200 μL MZ buffer (Tiangen, China) into each well. Thereafter, the total RNA was extracted using a miRNA isolation kit (Tiangen, China) following the manufacturer's protocol and quantified by a NanoDrop spectrophotometer (NanoDrop2000, Thermo Fisher Scientific, USA). The extracted RNA was reversely transcribed into cDNA with a QuantScript RT kit (Tiangen, China). The expression levels of relative genes combined with SYBR Green Supermix (Bio-Rad, USA) were measured using real-time quantitative polymerase chain reaction (RT-qPCR; CFX96 Touch, Bio-Rad, USA). The primers employed were listed in Table S1.

2.4.4 Immunofluorescent staining

Inducible nitric oxide synthase (iNOS) and arginase-1 (Arg-1) were selected as surface markers for M1 and M2 macrophages, respectively. The cells were fixed with 4% paraformaldehyde for 30 min, treated with 1% Triton X-100 solution for 5 min and then blocked with 10% goat serum for 2 h. After that, the cells were incubated with iNOS (1:500, Abcam, USA) and Arg-1 primary antibody (1:200, Abcam, USA) at 37 °C for 12 h, and then treated with the secondary antibody solution containing Alexa Fluor 488 (1:200, Abcam, USA) and Alexa Fluor 594 (1:200, Abcam, USA) for 30 min. The nuclei were stained with DPAI for 30 s. The specimens were characterized using a LCM.

2.5 *In vitro* macrophage-mediated osteogenesis

2.5.1 Cell proliferation

The proliferation of SaOS-2 cells was tested as described in section 2.4.1.

2.5.2 Alkaline phosphatase (ALP) activity

After culturing for 7 days, SaOS-2 cells were washed twice with PBS and lysed in 300 μL RIPA lysis buffer (Beyotime, China) for 15 min at 4 °C. The suspensions were collected and centrifuged for 10 min at 12, 000 rpm. The total protein content was measured using a BCA protein assay (Beyotime, China). The ALP activity was determined by an ALP testing kit (Beyotime, China) according to the manufacture's protocol and normalized by the measured protein content. For the staining of ALP activity, SaOS-2 cells were fixed by 4%

paraformaldehyde and stained by a BCIP/NBT alkaline phosphatase color development kit (Beyotime, China). The images were taken under an optical microscope.

2.5.3 Collagen secretion

After culturing for 7 and 10 days, the cells were fixed, stained by sirius red (Solarbio,China) for 16 h and photographed by optical microscopy. Subsequently, the dyes were dissolved in a mixed solution composed of 0.2 M NaOH and methanol at a volume ratio of 1:1. The OD values were measured by a multimode plate reader at 520 nm.

2.5.4 Matrix mineralization

For *in vitro* mineralization, each kind of MCM was further supplemented with 10 mM β-sodium glyceryl phosphate, 50 μg/mL vitamin C and 100 nM dexamethasone. After culturing for 7 and 14 days, the cells fixed and stained with 2% alizarin red solution (Solarbio, China) for 30 min. After washing for 3 times, the specimens were photographed using optical microscopy and then dissolved in 10% cetylpyridinium chloride solution. The OD values were measured by a multimode plate reader at 520 nm.

2.6 Statistical analysis of data

The results were generated from at least 3 three repetitions and expressed as mean ± standard deviation. The data were statistically analyzed using least significant difference (LSD) method. * $P < 0.05$ and ** $P < 0.01$ were considered to be significantly different.

3. Results

3.1 The physicochemical properties of various surfaces

3.1.1 Surface morphology and wettability

Fig. 1a exhibited the morphological features of various surfaces. Shallow pits (indicated by the blue dotted lines) were observed on Ti surface after acid etching. After subsequent alkali-heat treatment, ion exchange and heat treatment, nano-structures were further introduced onto AE-Ti surface. The morphological features of nano-structures were adjustable by altering the concentrations of NaOH solutions during the process of alkali-heat treatment. Nano-flakes, nano-flakes mixed with nano-wires and nano-wires were observed in AH0.5-, AH3- and AH5-Ti group, respectively. As shown in Fig. 1b, the AH0.5-Ti surface was mainly composed of Ti and O. The content of Na on AH0.5-Ti surface was within the measurement error of EDS technique, indicating that the presence of Na could be ignored.

The surface roughness of AE-Ti was measured to be around 1.38 μm (Fig. 1c), while the roughness values in AH0.5-, AH3- and AH5-Ti group were 1.53, 1.87 and 1.99 μm, respectively. This suggests that the AE-Ti possessed micro-scale surface topography. Moreover, the

introduction of nano-structures enhanced the roughness in sub-micron scale. The micro-scale pits combined with nano-structures could be perceived as typical micro/nano-structured features on Ti surfaces. As shown in Fig. 1d, micro/nano-structured Ti surfaces possessed significantly higher hydrophilicity compared to micro-structured Ti surface. Compared to those of AH0.5- and AH5-Ti surface, the water contact angle of AH3-Ti surface was even lower.

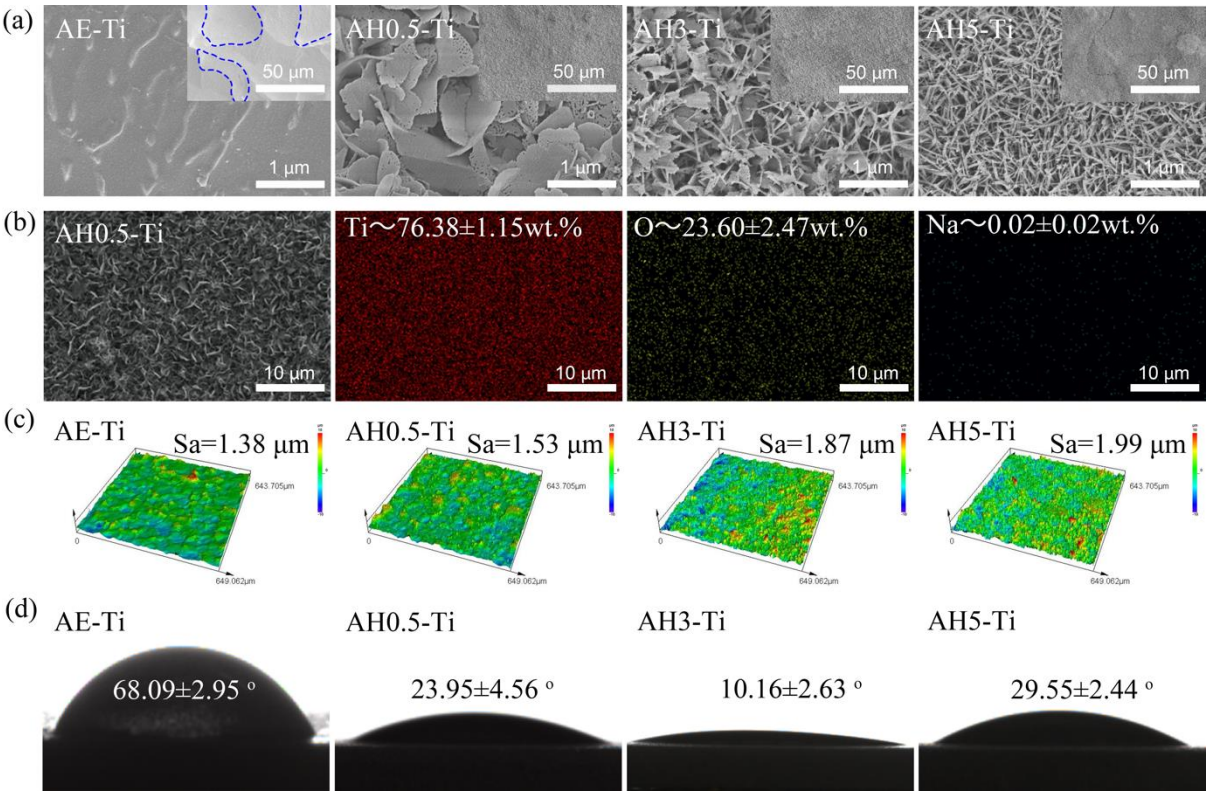

Fig. 1 (a) The surface morphology of various specimens, (b) the elemental composition of AH0.5-Ti surface analyzed by EDS as well as the measured (c) surface roughness and (d) wettability.

3.1.2 Phase and chemical composition

As shown in Fig. 2a, only α-Ti peaks (JCPDF No. 44-1294) were detected in AE-Ti group. After alkali-heat treatment, ion exchange and heat treatment, additional peaks corresponding to anatase (JCPDF No. 21-1272) and rutile (JCPDF No. 21-1276) phase of TiO_2 were found in AH0.5-, AH3- and AH5-Ti group. The presence of anatase was more predominant than that of rutile according to the peak intensity. This is probably because that the anatase phase could irreversibly transfer to rutile at 550 °C, even though this process is extremely slow [25].

The chemical composition of each surface was analyzed by XPS technique. As shown in Fig. 2b, the full spectra revealed that all surface were composed of C, O and Ti. The C1s peaks

located at 284.6 eV and 288.2 eV could be attributed to CO_2 presented in XPS device and adsorbed on specimen surfaces. For the spectra of Ti, two peaks located at 458.5 eV and 464.2 eV indicated the presence of TiO_2. The peaks of O, which were located at 529.7 eV and 531.6 eV, were considered to be corresponding to the lattice oxygen in TiO_2 and surface hydroxyl oxygen, respectively.

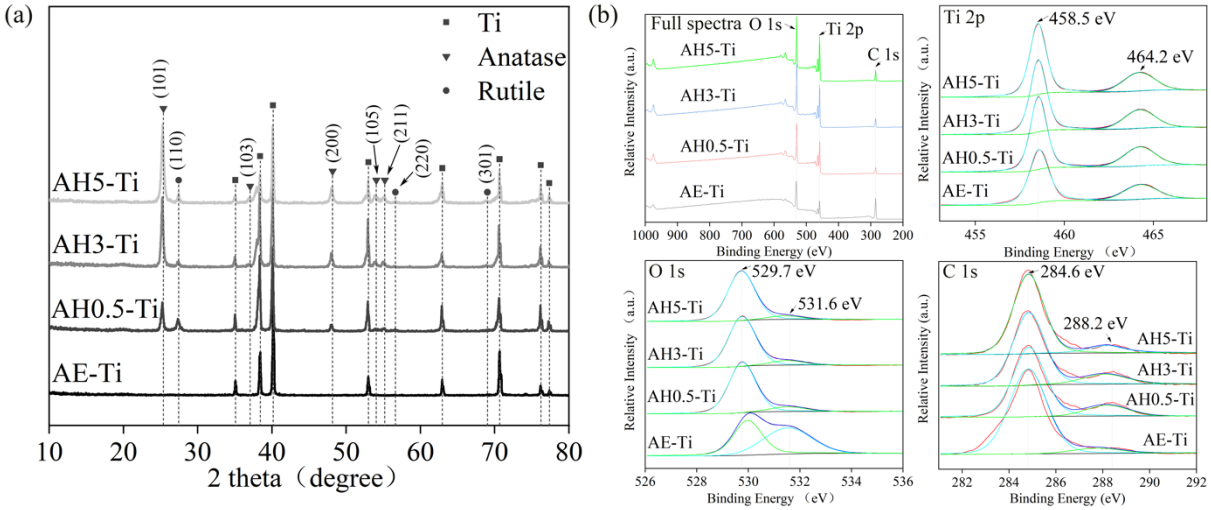

Fig. 2 The (a) XRD patterns and (b) XPS spectra of various surfaces.

3.2 Macrophage response to various surfaces

3.2.1 Cell morphology

As shown in Fig. 3a, the morphology of macrophages was highly dependent on Ti surface features. On AE-Ti surface, the macrophages were more polygonal in shape. Both lamellipodia (red arrows) and filopodia (white arrows) were found in AE-Ti group. On both AH0.5- and AH3-Ti surface, the macrophages were stellated and the extension of lamellipodia was observed. Compared to those on AH0.5-Ti surface, the macrophages in AH3-Ti group formed more filopodia. On AH5-Ti surface, pancake-shaped macrophages with the extension of numerous filopodia were noticed. The morphological features of macrophages grown on various surfaces were quantitatively analyzed based on the LCM images. As shown in Fig. 3b and c, the spreading area and major axis/minor ratio values of macrophages in different groups were comparable ($p > 0.05$), indicating that the morphological features of macrophages in response to various surfaces could not be simply described by their spreading areas and major axis/minor ratios.

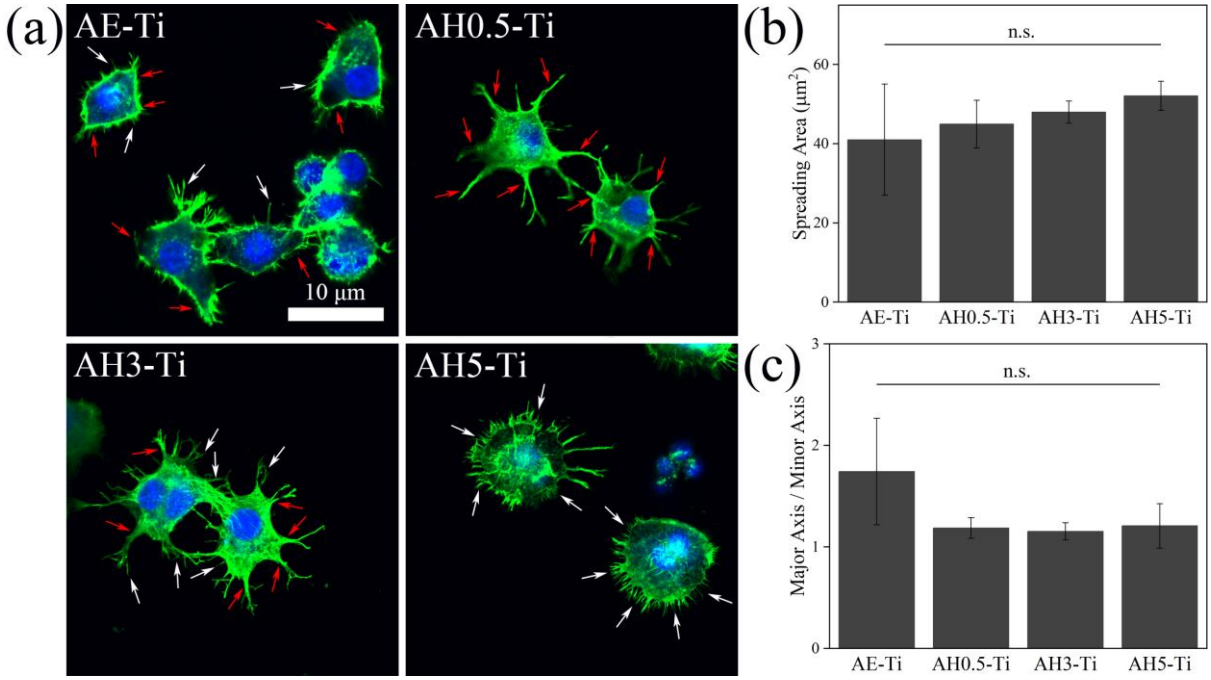

Fig. 3 The (a) morphology of macrophages grown on various surfaces for 2 days as well as quantitative analysis of cell morphological features including (b) spreading area and (c) ratio of major axis/minor axis. The red and white arrows indicated the presence of lamellipodia and filopodia, respectively. In addition, n.s. is noted for no significance ($p > 0.05$).

3.2.2 Macrophage proliferation

As shown in Fig. 4, the degrees of macrophage viability on various surfaces were comparable. As AE-Ti surface is well-known for its cyto-compatibility, the micro/nano-structured Ti surfaces could also be considered to be cyto-compatible.

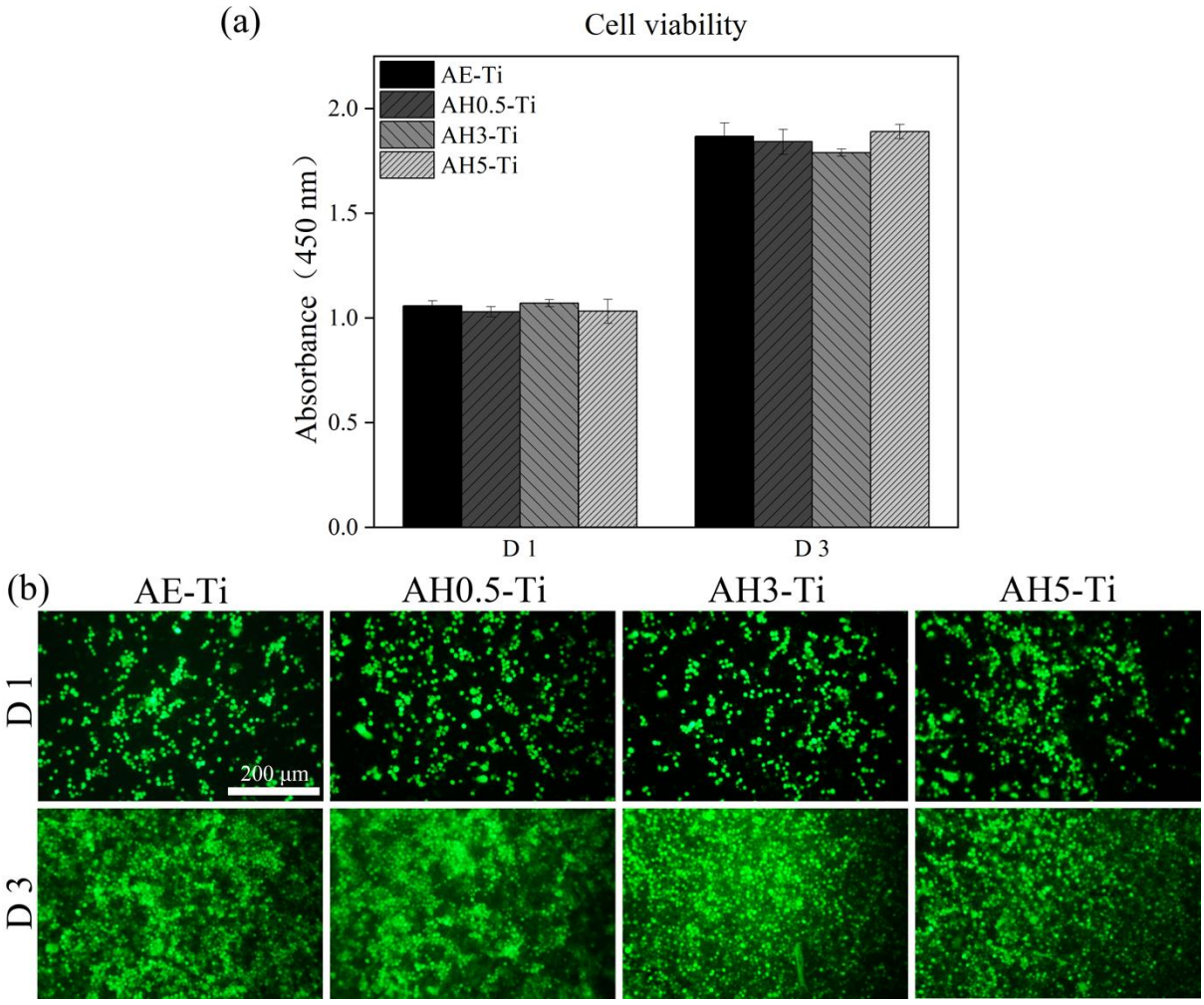

Fig. 4 The proliferation of macrophages grown on various surfaces for 1 and 3 days evaluated by (a) CCK-8 assay and (b) live cell staining.

3.2.3 Macrophage polarization

The polarization behavior of macrophages in response to various surfaces was analyzed by RT-qPCR technique. As shown in Fig. 5, micro/nano-structured Ti surfaces tended to polarize macrophages to their M2 phenotype compared to micro-structured Ti surface. This is evidenced by the down-regulated expressions of pro-inflammatory genes including iNOS (Fig. 5a), CD86 (Fig. 5b) and TNF-α (Fig. 5d) as well as up-regulated anti-inflammatory gene expressions including CD206 (Fig. 5c), IL-10 (Fig. 5f) and CCL-24 (Fig. 5g) in AH0.5-, AH3- and AH5-Ti group. Among micro/nano-structured Ti surfaces, only AH0.5-Ti surface decreased the gene expression of IL-1β (Fig. 5e) compared to control. This suggests that the gene expression of IL-1β is less sensitive to nano-structures compared to that of TNF-α. It is worthy of mentioning that gene expressions of IL-10 (Fig. 5f) and CCL-24 (Fig. 5g) were significantly higher in AH3-Ti group compared those in AH0.5- and AH5-Ti group, indicating that AH3-Ti surface

exhibited the strongest anti-inflammatory effect. The gene expressions of osteogenic growth factors were basically enhanced on micro/nano-structured Ti surface compared to micro-structured Ti surface, with AH3-Ti surface exhibited the strongest stimulatory effects (Fig. 5h-j).

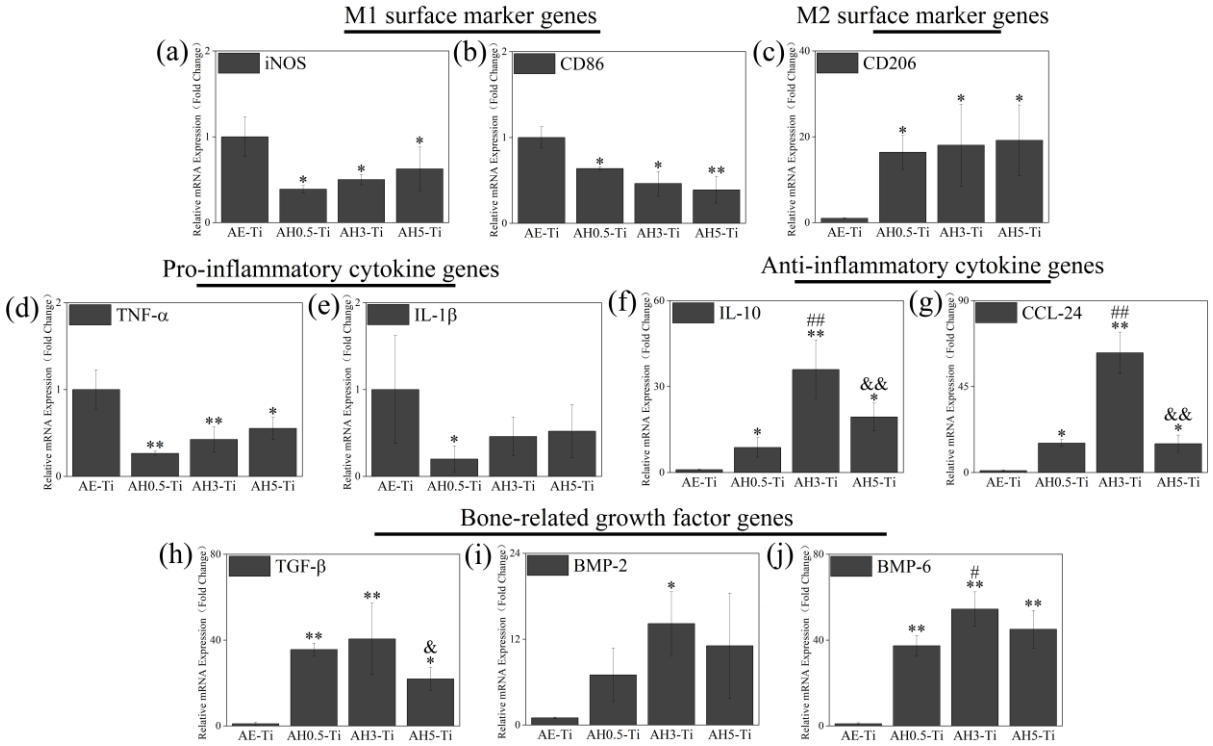

Fig. 5 The gene expression levels of (a) iNOS, (b) CD86, (c) CD206, (d) TNF-α, (e) IL-1β, (f) IL-10, (g) CCL-24, (h) TGF-β, (i) BMP-2 and (j) BMP-6 in macrophages grown on various surfaces for 2 days. *$p < 0.05$ and **$p < 0.01$ indicate the presence of significant differences between AE-Ti and other groups, #$p < 0.05$ and ##$p < 0.01$ indicate the presence of significant differences between AH0.5-Ti and other groups, &$p < 0.05$ and &&$p < 0.01$ indicate the presence of significant differences between AH3-Ti and other groups.

The activation state of macrophages was also investigated at protein-level using immunofluorescent staining method. As shown in Fig. 6, AE-Ti surface significantly promoted the expression of iNOS compared other groups. However, the expressions of Arg-1 were higher on micro/nano-structured surfaces, with AH3-Ti surface showing the highest Arg-1expression level. The immunofluorescent staining results were consistent with those obtained by RT-PCR technique.

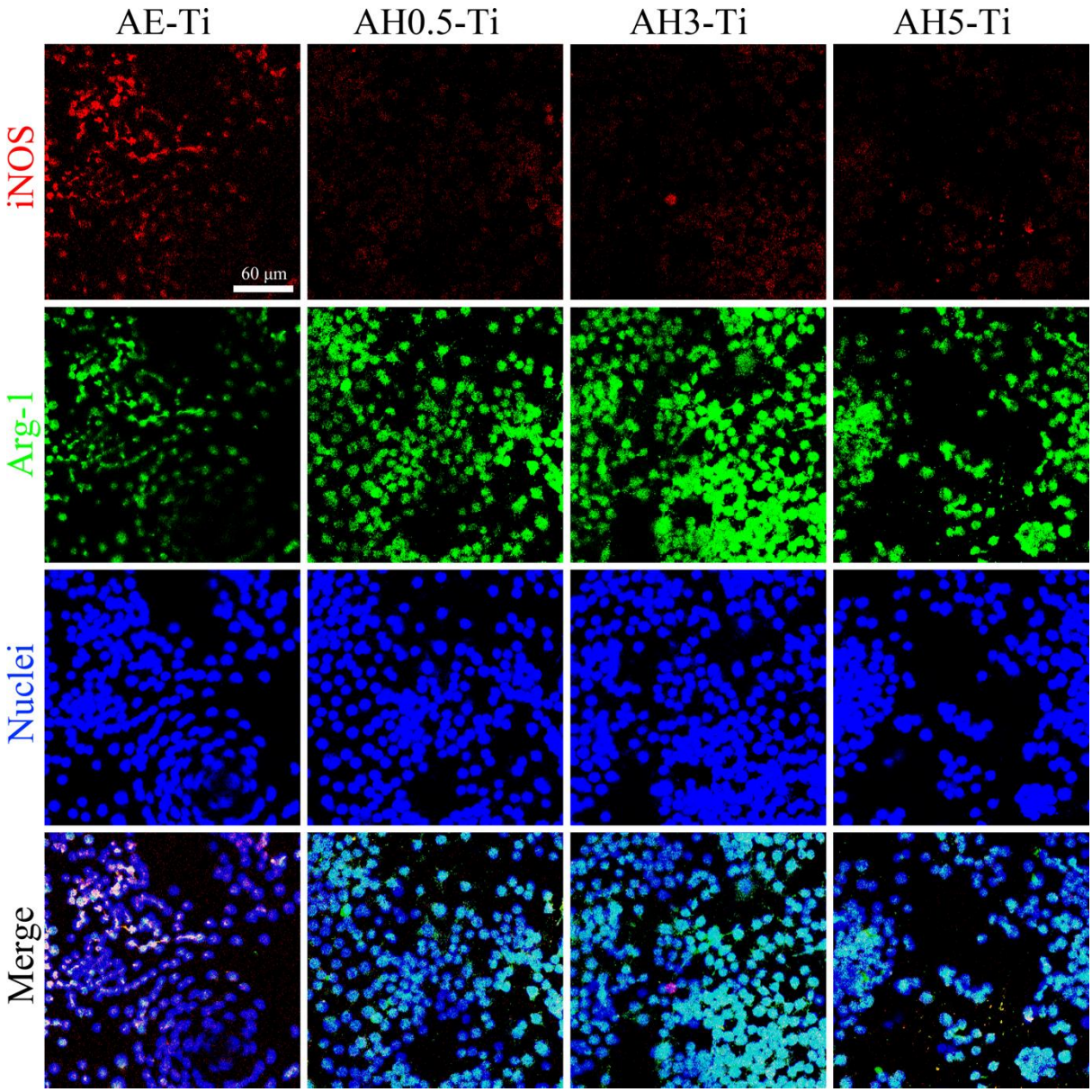

Fig. 6 Immunofluorescent staining results showing the expression levels of iNOS (red) and Arg-1 (green) in macrophages in response to various surfaces with cell nuclei stained in blue.

3.3 *In vitro* Macrophage-mediated osteogenesis

3.3.1 Osteoblast proliferation

As shown in Fig. 7, the proliferation of SaOS-2 cells was enhanced in AH0.5-, AH3- and AH5-MCM group on day 4 and 6 compared to control, even though AH0.5- and AH3-MCM did not promoted cell proliferation on day 2.

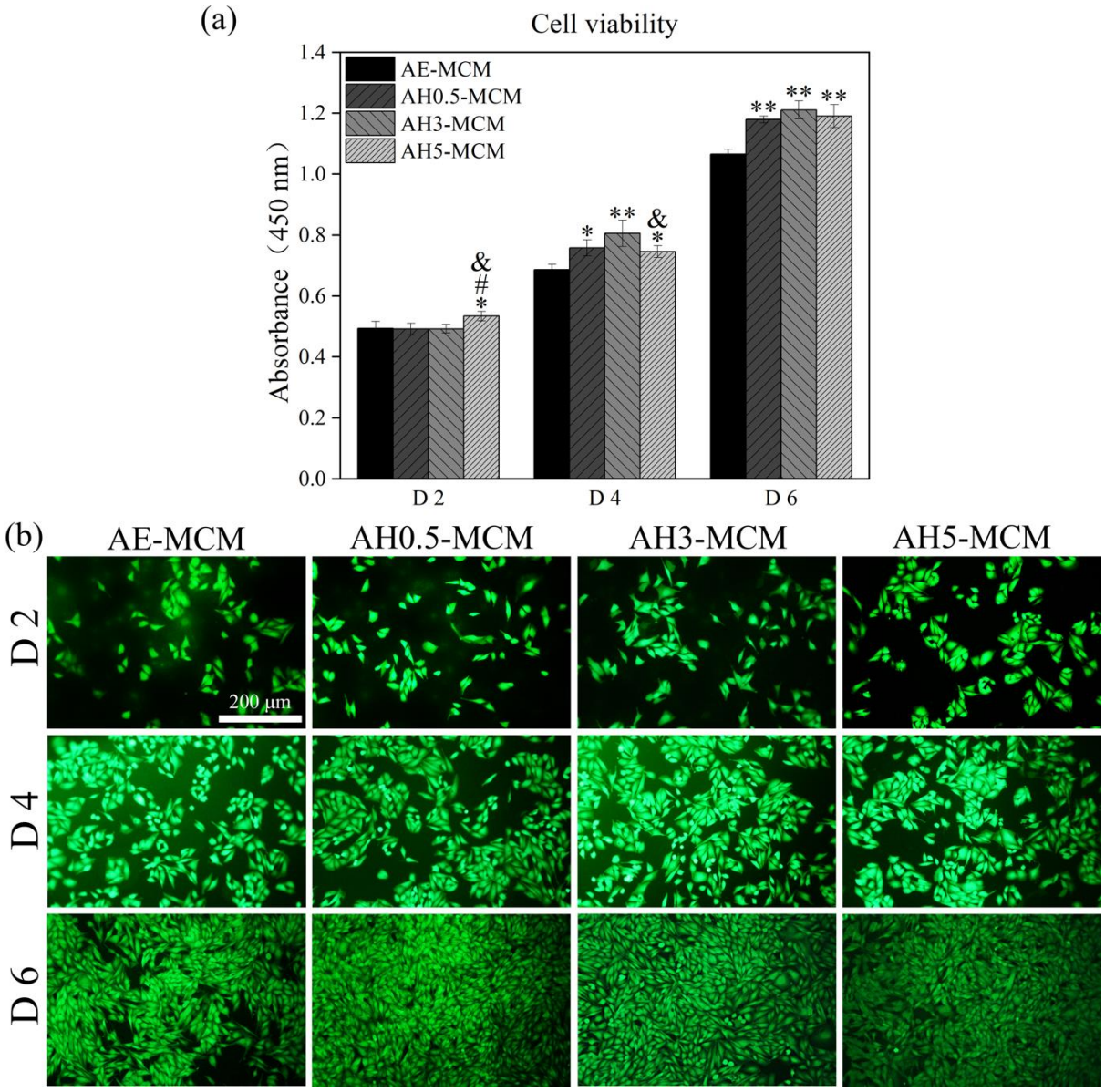

Fig. 7 The proliferation of osteoblasts cultured by various MCM for 2, 4 and 6 days evaluated by (a) CCK-8 assay and (b) live cell staining. *p < 0.05 and **p < 0.01 indicate the presence of significant differences between AE-MCM and other groups, #p <0.05 and ##p < 0.01 indicate the presence of significant differences between AH0.5-MCM and other groups, &p < 0.05 and &&p < 0.01 indicate the presence of significant differences between AH3-MCM and other groups.

3.3.2 Osteoblast differentiation

The differentiation of SaOS-2 cells in response to various MCM was characterized by ALP activity, collagen production and *in vitro* mineralization. As shown in Fig. 8a, AH3-MCM promoted the ALP activity in SaOS-2 cells compared to other MCM. The secretion of collagen was enhanced in AH0.5- and AH3-MCM group on day 7 (Fig. 8b). Till day 10, the collagen

secretion was strong in AH0.5- and AH3-MCM group, mild in AH5-MCM group and weak in AE-MCM group (Fig. 8b). As shown in Fig. 8c, the *in vitro* mineralization on day 7 and 14 mainly followed the trend: AH3-MCM > AH5-MCM ≈ AH0.5-MCM > AE-MCM.

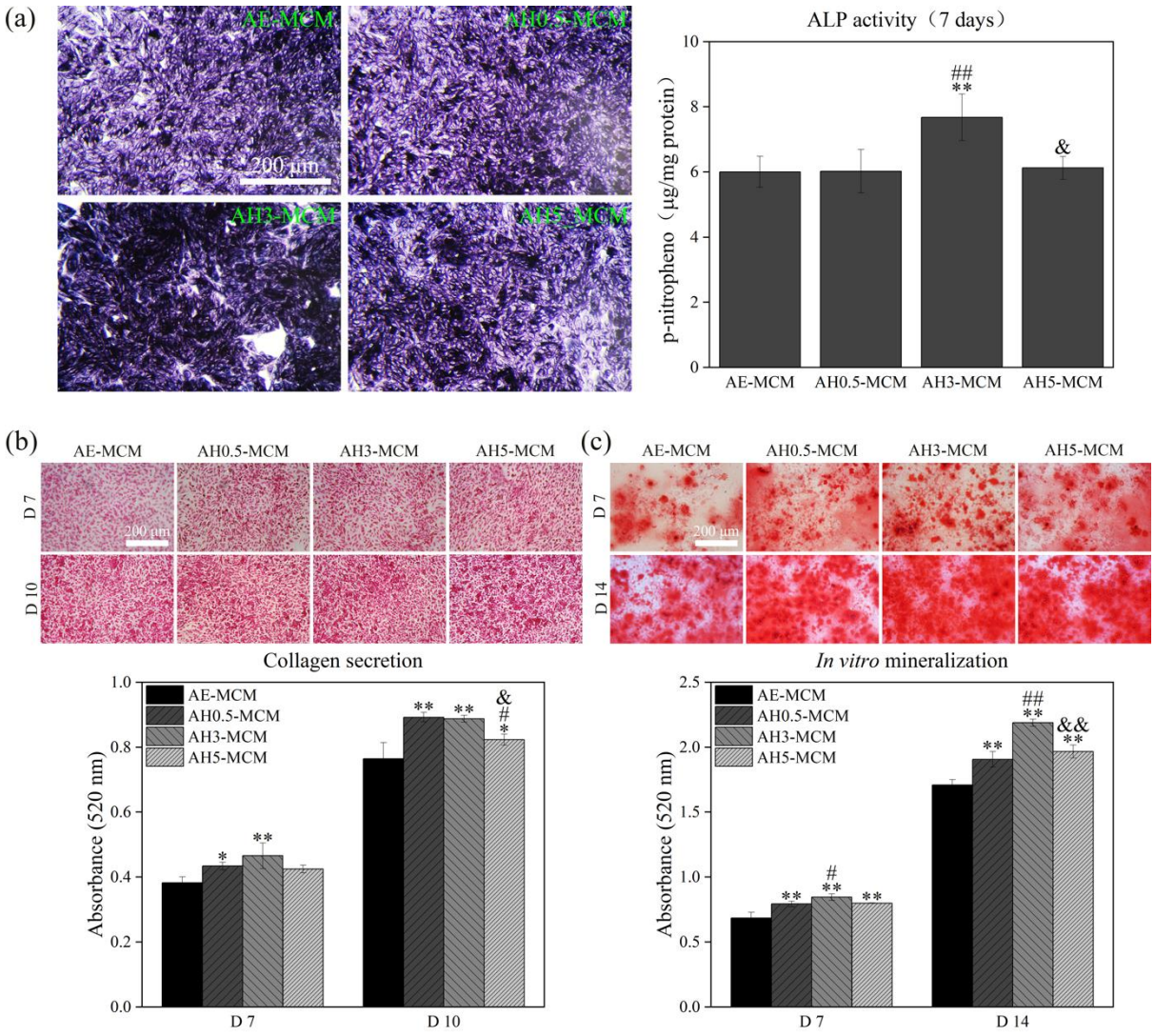

Fig. 8 The (a) ALP activity, (b) collagen secretion and (c) *in vitro* mineralization of SaOS-2 cells incubated in various MCM. *p < 0.05 and **p < 0.01 indicate the presence of significant differences between AE-MCM and other groups, #p <0.05 and ##p < 0.01 indicate the presence of significant differences between AH0.5-MCM and other groups, &p < 0.05 and &&p < 0.01 indicate the presence of significant differences between AH3-MCM and other groups.

4. Discussions

Understanding the interactions between micro/nano-structured surfaces and macrophages is essential for the development of inflammation-modulatory Ti-based implants. In the current

work, various nano-structures were introduced onto AE-treated micro-structured Ti surface through alkali-heat treatment. To decouple the influence of surface topography and chemistry on cell response, the alkali-heat treated micro/nano-structured Ti surfaces were further soaked in HCl solution for ion exchange. After that, a subsequent heat treatment process was employed to modulate the phase composition.

4.1 The formation mechanism of micro/nano-structured Ti surfaces

During the process of acid etching, the acids could firstly dissolve the protective TiO_2 film and subsequently corrode Ti substrate, thus resulting in chemical texturing of Ti surface. After the treatment, a naturally formed TiO_2 passivation layer will soon cover Ti surface again [26]. This is confirmed by the XPS spectra of AE-Ti presented in Fig. 2b. During alkali-heat treatment, the superficial TiO_2 layer of AE-Ti could react with Na^+ and OH^- within NaOH solution to form $Na_2Ti_3O_7$ [27]. With increased concentration of NaOH solution, the nucleation of $Na_2Ti_3O_7$ crystals could be enhanced, while their growth is speculated to be inhibited due to the consumption of TiO_2 and reactive ions during the nucleation process [28]. Thus, the AE-Ti surface treated by NaOH solution with low concentration (0.5 M) formed larger, but less nano-structures than that treat by high concentration NaOH solution (5M). Similarly, the surface treated by 3M NaOH solution exhibited both features of nano-flakes and nano-wires (Fig. 1a) [28]. During the process of ion exchange, H^+ could replace Na^+ within $Na_2Ti_3O_7$ in HCl solution and lead to the formation of $H_2Ti_3O_7$. Consistently, no signal of Na was detected on micro/nano-structured Ti surface by XPS technique (Fig. 2b). Thereafter, $H_2Ti_3O_7$ could further transform to TiO_2 after heat treatment, evidenced by the XRD results presented in Fig. 2a. Together, the chemical reactions involved in the preparation process of nano-structures on AE-Ti surface could be listed as below:

Alkali-heat treatment: $3TiO_2 + 2Na^+ + 2OH^- \rightarrow Na_2Ti_3O_7 + H_2O$

Ion exchange: $Na_2Ti_3O_7 + 2H^+ \rightarrow H_2Ti_3O_7 + 2Na^+$

Heat treatment: $H_2Ti_3O_7 \rightarrow 3TiO_2 + H_2O$

The wettability of a solid surface is well-known to be mainly determined by two factors including surface topography and energy [29]. In this work, various specimen surfaces were similar in chemical and phase composition. Thus, the surface topography is considered as a major factor that influence material surface wettatbility. As discussed above, as-prepared micro- and micro/nano-structured Ti surfaces possessed similar surface chemical and phase compositions, while different surface topographies. Therefore, they are suitable models for the investigation of the modulatory roles of micro/nano-structured surfaces on macrophage response.

4.2 Macrophage response to various surfaces

The results presented in this work revealed that micro/nano-structured Ti surfaces significantly modulated the morphology and polarization of macrophages, while rarely changed cell proliferation. As various surfaces possessed similar surface chemistry, their surface topographies were considered as the major factor in determining macrophage attachment and polarization.

Previous investigations reported that micro/nano-structured surfaces could significantly modulate cell adhesion by providing different contact areas between cells and surfaces [30-33]. As shown in Fig. 3a, the macrophages were polygonal on micro-structured Ti surface. This is probably because that the cytoskeletons of macrophages could fully contact with the profiles of shallow pits (Fig. 9). Consistently, macrophages grown on smooth or micro-roughened Ti surfaces were previously reported to be polygon-shaped [34, 35]. With the presence of nano-structures, the contact areas between macrophages and surfaces are considered to be significantly confined. On AH5 Ti surface, the macrophages extended numerous filopodia to search for suitable positions for adhesion [36]. However, these filopodia did not transform to lamellipodia because the nano-wires could not provide sufficient areas for macrophages to form stable adhesion (Fig. 9). Differently, the nano-flakes could provide relatively larger areas for macrophage adhesion. Therefore, more lamellipodia were found on AH0.5-Ti surface (Fig. 3). The macrophages were stellate on AH0.5-Ti surface because their cytoskeletons could not fully contact with the profiles of nano-flakes (Fig. 9). These results suggest that the nano-flakes and nano-wires are beneficial for the formation of lamellipodia and filopodia, respectively. Consistently, both lamellipodia and filopodia were found to be obvious on AH3-Ti surface, which possessed mixed surface features of nano-flakes and nano-wires (Fig. 3).

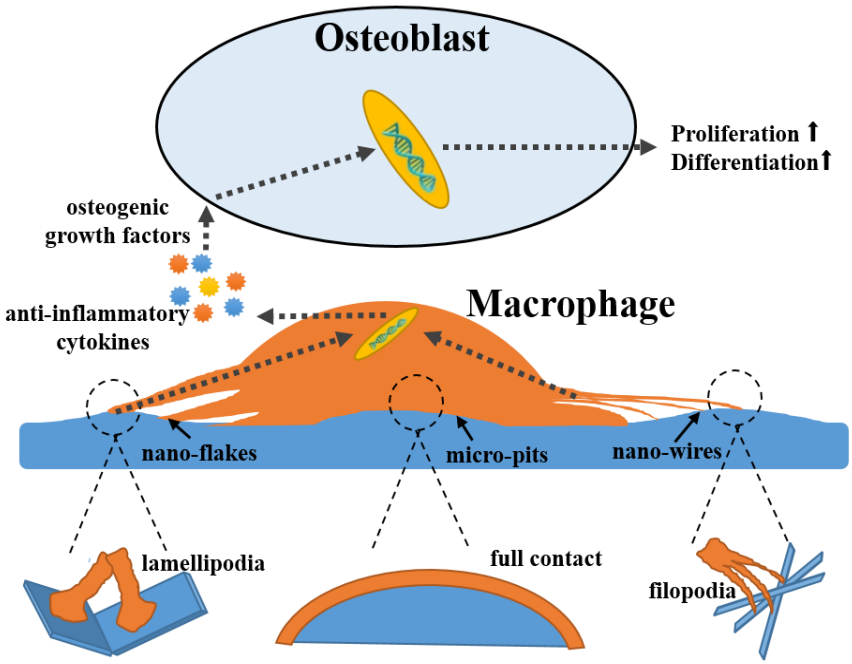

Fig. 9 Schematic showing the interactions between micro/nano-structured surfaces and macrophages as well as macrophage-mediated osteogenesis.

The polarization state of macrophages is closely related to their morphology [37]. McWhorter et al. reported that M0, M1 and M2 macrophages were spherical, polygonal and spindle-like, respectively [38]. However, Chen et al. recently found that roundish macrophages modulated by nano-porous surfaces exhibited a more anti-inflammatory phenotype [39]. These results suggest that the correlation between macrophage morphology and polarization is still controversial. In the current work, stellate and roundish macrophages with the extension of lamellipodia and/or filopodia were more anti-inflammatory compared to polygonal macrophages. This indicates that the morphological feature of macrophages could not be regarded as a single indicator for macrophage phenotype. However, it is reasonable to speculate that the nano-structures could modulate the arrangement of macrophage cytoskeleton and thus influence macrophage activation. In addition, the macrophages grown on AH3-Ti surface were found to be more anti-inflammatory compared to those grown on AH0.5-Ti and AH5-Ti surface, suggesting that the nano-flakes and nano-wires could play a synergistic role in inducing M2 phenotype of macrophages. However, the underlying mechanisms are still needed to be explored. The results suggest that introducing nano-structures on micro-structured Ti surfaces could be a promising strategy to modulate macrophage response.

It is worthy of mentioning that the wettability of biomaterial surfaces could also modulate cellular response. Lv et al. recently reported that a hydrophilic flat surface promoted M2

polarization in macrophages by modulating the interaction between integrin β1 and adsorbed fibronectin [40]. Different from a flat surface which modulates protein adhesion due to its wettability, micro/nano-structured surfaces interact with proteins in a more complex way. The nano-structures of micro/nano-structured surfaces could modulate the conformation and distribution of absorbed proteins in a surface morphology-dependent manner, which subsequently influence cellular response. In addition, the wettability evaluated by contact angle measurement reflects the interactions between a water-drop and material surface at macro-scale, while cannot reflect protein-surface interactions at nano-scale. Thus, the surface topography of micro/nano-structured surfaces is considered to be more important than the surface wettability in modulating cellular response. Although RAW 264.7 cells are commonly employed cell model for macrophages, they are different from primary macrophages to some extent. Therefore, further investigations carried out using primary macrophages such as peripheral blood mononuclear cell (PBMC)-derived and bone marrow-derived macrophages are still needed.

4.3 Macrophage-mediated osteogenesis

The proliferation of SaOS-2 cells on day 6 was enhanced in AH3-, AH5- and AH0.5-MCM group compared to that in AE-MCM group, suggesting that an anti-inflammatory micro-environment is favorable for osteoblast proliferation. The differentiation of osteoblasts in response to various MCM basically followed the trend: AH3-MCM > AH5-MCM ≈ AH0.5-MCM > AE-MCM. This trend is consistent with the release profiles of osteogenic growth factors from macrophages grown on various surfaces. At physiological concentration, TGF-β can induce matrix mineralization like dexamethasone [41]. In addition, BMPs are well-known for their stimulatory roles on the osteogenic differentiation of MSCs and osteoblast maturation [42-44]. Luo et al. compared the osteogenic potential of 14 human BMPs and found that BMP-2, 6, and 9 are the most effective inducers of osteogenesis *in vitro* and *in vivo* [44]. The promoted osteoblast differentiation in micro/nano-structured Ti groups compared to that on micro-structured Ti surface could be owing to the enhanced gene expressions of TGF-β and BMP-6. Moreover, macrophages grown on AH3-Ti surface expressed higher level of BMP-6 compared to those grown on AH0.5- and AH5-Ti surface, which explained the further enhanced osteogenic potential of AH3-MCM. Consistently, Chen et al. found that M2 macrophages induced by calcium phosphate coated magnesium scaffold expressed higher levels of BMP-2 and vascular endothelial growth factor (VEGF) to stimulate the osteogenic differentiation of MSCs [45]. Fernandes et al. reported that macrophages in their M2 phenotype could promote the differentiation of MSCs [46]. Thus, inducing appropriate M2 phenotype in macrophages

via biomaterial surface engineering could be a promising approach for enhanced osteogenesis.

5. Conclusions

In this study, TiO_2 nano-structures were introduced onto acid-etched micro-structured Ti surfaces by alkali-heat treatment, ion exchange and subsequent heat treatment. The morphological features of nano-structures could be modulated by adjusting the concentration of NaOH solution during alkali-heat treatment. Both micro- and micro/nano-structured Ti surfaces possessed similar surface chemical and phase compositions. The morphology of macrophages was found to be highly dependent on the morphological features of nano-structures on micro-structured Ti surfaces. The macrophages grown on micro/nano-structured Ti surfaces were more anti-inflammatory and stronger in osteogenic potential compared to those grown on micro-structured Ti surface. Compared to AH0.5- and AH5-Ti surface, AH3-Ti surface which possessed mixed features of nano-flakes and nano-wires exhibited the strongest anti-inflammatory and osteoimmunomodulatory effects. The results suggest that introducing nano-structures on micro-structured Ti surfaces could be a promising strategy to modulate macrophage response.

CRediT authorship contribution statement

Wentao Liu: Data curation, Investigation, Writing – Original draft. **Luxin Liang:** Data curation, Formal analysis. **Dapeng Zhao:** Data curation. **Yingtao Tian:** Data curation. **Bo Liu:** Writing – review & editing. **Qianli Huang:** Coceptualization, Methodology, Supervision, Writing – review & editing. **Hong Wu:** Coceptualization, Methodology, Supervision, Writing – review & editing.

Declaration of competing interest

The authors declare that they have no known competing financial interests or personal relationships that could have appeared to influence the work reported in this paper.

Acknowledgments

This work was supported by the National Natural Science Foundation of China (Grant No. 51771233, 52071346, and 51604104), Fundamental Research Funds for the Central Universities of Central South University (Grant No. 2020zzts445), China Postdoctoral Science Foundation (Grant No. 2018M633164) and Guangdong Basic and Applied Basic Research Foundation (Grant No. 2019A1515110736).

References:

[1] S.M. Eskildsen, Z.J. Wilson, D.C. McNabb, C.W. Olcott, D.J. Del Gaizo, Acetabular Reconstruction With the Medial Protrusio Technique for Complex Primary and Revision Total Hip Arthroplasties, J Arthroplasty, 32 (2017) 3474-3479.

[2] R.A. Gittens, R. Olivares-Navarrete, Z. Schwartz, B.D. Boyan, Implant osseointegration and the role of microroughness and nanostructures: Lessons for spine implants, Acta biomaterialia, 10 (2014) 3363-3371.

[3] F. Loi, L.A. Córdova, J. Pajarinen, T.-h. Lin, Z. Yao, S.B. Goodman, Inflammation, fracture and bone repair, Bone, 86 (2016) 119-130.

[4] H. Takayanagi, Osteoimmunology: shared mechanisms and crosstalk between the immune and bone systems, Nature Reviews Immunology, 7 (2007) 292-304.

[5] J. Pajarinen, T. Lin, E. Gibon, Y. Kohno, M. Maruyama, K. Nathan, L. Lu, Z. Yao, S.B. Goodman, Mesenchymal stem cell-macrophage crosstalk and bone healing, Biomaterials, 196 (2019) 80-89.

[6] Z. Chen, T. Klein, R.Z. Murray, R. Crawford, J. Chang, C. Wu, Y. Xiao, Osteoimmunomodulation for the development of advanced bone biomaterials, Materials Today, 19 (2015) 304-321.

[7] D.M. Mosser, J.P. Edwards, Erratum: Exploring the full spectrum of macrophage activation, Nature Reviews Immunology, 10 (2010) 460-460.

[8] V. Malheiro, F. Lehner, V. Dinca, P. Hoffmann, K. Maniura, Convex and concave micro-structured silicone controls the shape, but not the polarization state of human macrophages, Biomater. Sci., 4 (2016).

[9] T.J. Koh, L.A. DiPietro, Inflammation and wound healing: the role of the macrophage, Expert Rev Mol Med, 13 (2011) e23.

[10] S.K. Biswas, A. Mantovani, Macrophage plasticity and interaction with lymphocyte subsets: cancer as a paradigm, Nat Immunol, 11 (2010) 889-896.

[11] Q. Huang, Z. Ouyang, Y. Tan, H. Wu, Y. Liu, Activating macrophages for enhanced osteogenic and bactericidal performance by Cu ion release from micro/nano-topographical coating on a titanium substrate, Acta biomaterialia, 100 (2019) 415-426.

[12] Y. Xie, C. Hu, Y. Feng, D. Li, T. Ai, Y. Huang, X. Chen, L. Huang, J. Tan, Osteoimmunomodulatory effects of biomaterial modification strategies on macrophage polarization and bone regeneration, Regenerative Biomaterials, 7 (2020) 233-245.

[13] H. Wu, Y. Yin, X.B. Hu, C. Peng, Y. Liu, Q.X. Li, W.D. Huang, Q.L. Huang, Effects of Environmental pH on Macrophage Polarization and Osteoimmunomodulation, Acs Biomaterials Science & Engineering, 5 (2019) 5548-5557.
[14] X. Liu, P.K. Chu, C. Ding, Surface modification of titanium, titanium alloys, and related materials for biomedical applications, Materials Science and Engineering: R: Reports, 47 (2004) 49-121.
[15] X.Z. Li, Q.L. Huang, X.B. Hu, D.K. Wu, N.F. Li, Y. Liu, Q.X. Li, H. Wu, Evaluating the osteoimmunomodulatory properties of micro-arc oxidized titanium surface at two different biological stages using an optimized in vitro cell culture strategy, Materials Science & Engineering C-Materials for Biological Applications, 110 (2020).
[16] X. Shen, P. Ma, Y. Hu, G. Xu, J. Zhou, K. Cai, Mesenchymal stem cell growth behavior on micro/nano hierarchical surfaces of titanium substrates, Colloids and Surfaces B: Biointerfaces, 127 (2015) 221-232.
[17] W.-G. Bae, J. Kim, Y.-H. Choung, Y. Chung, K.Y. Suh, C. Pang, J.H. Chung, H.E. Jeong, Bio-inspired configurable multiscale extracellular matrix-like structures for functional alignment and guided orientation of cells, Biomaterials, 69 (2015) 158-164.
[18] D.J. Kyle, A. Oikonomou, E. Hill, A. Bayat, Development and functional evaluation of biomimetic silicone surfaces with hierarchical micro/nano-topographical features demonstrates favourable in vitro foreign body response of breast-derived fibroblasts, Biomaterials, 52 (2015) 88-102.
[19] L. Xia, K. Lin, X. Jiang, B. Fang, Y. Xu, J. Liu, D. Zeng, M. Zhang, X. Zhang, J. Chang, Effect of nano-structured bioceramic surface on osteogenic differentiation of adipose derived stem cells, Biomaterials, 35 (2014) 8514-8527.
[20] R.A. Gittens, R. Olivares-Navarrete, S.L. Hyzy, K.H. Sandhage, Z. Schwartz, B.D. Boyan, Superposition of nanostructures on microrough titanium–aluminum–vanadium alloy surfaces results in an altered integrin expression profile in osteoblasts, Connective tissue research, 55 (2014) 164-168.
[21] L. Bai, Y. Liu, Z. Du, Z. Weng, W. Yao, X. Zhang, X. Huang, X. Yao, R. Crawford, R. Hang, Differential effect of hydroxyapatite nano-particle versus nano-rod decorated titanium micro-surface on osseointegration, Acta biomaterialia, 76 (2018) 344-358.
[22] Y. Li, C. Yang, X. Yin, Y. Sun, J. Weng, J. Zhou, B. Feng, Inflammatory responses to micro/nano-structured titanium surfaces with silver nanoparticles in vitro, Journal of Materials Chemistry B, 7 (2019) 3546-3559.

[23] J. Luo, Y. He, F. Meng, N. Yan, Y. Zhang, W. Song, The Role of Autophagy in M2 Polarization of Macrophages Induced by Micro/Nano Topography, International Journal of Nanomedicine, 15 (2020) 7763.
[24] Y. He, J. Luo, Y. Zhang, Z. Li, F. Chen, W. Song, Y. Zhang, The unique regulation of implant surface nanostructure on macrophages M1 polarization, Materials Science and Engineering: C, 106 (2020) 110221.
[25] R. Arroyo, G. Cordoba, J. Padilla, V.H. Lara, Influence of manganese ions on the anatase-rutile phase transition of TiO2 prepared by the sol-gel process, Materials Letters, 54 (2002) 397-402.
[26] B.R. Chrcanovic, M.D. Martins, Study of the influence of acid etching treatments on the superficial characteristics of Ti, Materials Research, 17 (2014) 373-380.
[27] H.Y. Tian, G.H. Zhao, Y.N. Zhang, Y.B. Wang, T.C. Cao, Hierarchical (001) facet anatase/rutile TiO2 heterojunction photoanode with enhanced photoelectrocatalytic performance, Electrochimica Acta, 96 (2013) 199-205.
[28] X.Y. Deng, Q.L. Ma, Y.Q. Cui, X.W. Cheng, Q.F. Cheng, Fabrication of TiO2 nanorods/nanosheets photoelectrode on Ti mesh by hydrothermal method for degradation of methylene blue:influence of calcination temperature, Applied Surface Science, 419 (2017) 409-417.
[29] B. He, N.A. Patankar, J. Lee, Multiple equilibrium droplet shapes and design criterion for rough hydrophobic surfaces, Langmuir, 19 (2003) 4999-5003.
[30] W.L. Lu, N. Wang, P. Gao, C.Y. Li, H.S. Zhao, Z.T. Zhang, Effects of anodic titanium dioxide nanotubes of different diameters on macrophage secretion and expression of cytokines and chemokines, Cell Prolif, 48 (2015) 95-104.
[31] E. Saino, M.L. Focarete, C. Gualandi, E. Emanuele, A.I. Cornaglia, M. Imbriani, L. Visai, Effect of electrospun fiber diameter and alignment on macrophage activation and secretion of proinflammatory cytokines and chemokines, Biomacromolecules, 12 (2011) 1900-1911.
[32] E. Lamers, X.F. Walboomers, M. Domanski, L. Prodanov, J. Melis, R. Luttge, L. Winnubst, J.M. Anderson, H.J. Gardeniers, J.A. Jansen, In vitro and in vivo evaluation of the inflammatory response to nanoscale grooved substrates, Nanomedicine, 8 (2012) 308-317.
[33] Q. Huang, T.A. Elkhooly, X. Liu, R. Zhang, X. Yang, Z. Shen, Q. Feng, Effects of hierarchical micro/nano-topographies on the morphology, proliferation and differentiation of osteoblast-like cells, Colloids Surf B Biointerfaces, 145 (2016) 37-45.

[34] K.S. Tan, L. Qian, R. Rosado, P.M. Flood, L.F. Cooper, The role of titanium surface topography on J774A.1 macrophage inflammatory cytokines and nitric oxide production, Biomaterials, 27 (2006) 5170-5177.
[35] X. Li, Q. Huang, T.A. Elkhooly, Y. Liu, H. Wu, Q. Feng, L. Liu, Y. Fang, W. Zhu, T. Hu, Effects of titanium surface roughness on the mediation of osteogenesis via modulating the immune response of macrophages, Biomed Mater, 13 (2018) 045013.
[36] M.J. Dalby, N. Gadegaard, R.O. Oreffo, Harnessing nanotopography and integrin–matrix interactions to influence stem cell fate, Nature materials, 13 (2014) 558-569.
[37] S.W. Waldo, Y. Li, C. Buono, B. Zhao, E.M. Billings, J. Chang, H.S. Kruth, Heterogeneity of human macrophages in culture and in atherosclerotic plaques, Am J Pathol, 172 (2008) 1112-1126.
[38] F.Y. McWhorter, T. Wang, P. Nguyen, T. Chung, W.F. Liu, Modulation of macrophage phenotype by cell shape, Proc Natl Acad Sci U S A, 110 (2013) 17253-17258.
[39] Z. Chen, S. Ni, S. Han, R. Crawford, S. Lu, F. Wei, J. Chang, C. Wu, Y. Xiao, Nanoporous microstructures mediate osteogenesis by modulating the osteo-immune response of macrophages, Nanoscale, 9 (2017) 706-718.
[40] L. Lv, Y.T. Xie, K. Li, T. Hu, X. Lu, Y.Z. Cao, X.B. Zheng, Unveiling the Mechanism of Surface Hydrophilicity-Modulated Macrophage Polarization, Advanced Healthcare Materials, 7 (2018).
[41] L. Rifas, T-cell cytokine induction of BMP-2 regulates human mesenchymal stromal cell differentiation and mineralization, J Cell Biochem, 98 (2006) 706-714.
[42] Z.H. Deng, Y.S. Li, X. Gao, G.H. Lei, J. Huard, Bone morphogenetic proteins for articular cartilage regeneration, Osteoarthritis Cartilage, 26 (2018) 1153-1161.
[43] C.M. Kemmis, A. Vahdati, H.E. Weiss, D.R. Wagner, Bone morphogenetic protein 6 drives both osteogenesis and chondrogenesis in murine adipose-derived mesenchymal cells depending on culture conditions, Biochem Biophys Res Commun, 401 (2010) 20-25.
[44] X. Luo, J. Chen, W.X. Song, N. Tang, J. Luo, Z.L. Deng, K.A. Sharff, G. He, Y. Bi, B.C. He, E. Bennett, J. Huang, Q. Kang, W. Jiang, Y. Su, G.H. Zhu, H. Yin, Y. He, Y. Wang, J.S. Souris, L. Chen, G.W. Zuo, A.G. Montag, R.R. Reid, R.C. Haydon, H.H. Luu, T.C. He, Osteogenic BMPs promote tumor growth of human osteosarcomas that harbor differentiation defects, Lab Invest, 88 (2008) 1264-1277.
[45] Z. Chen, X. Mao, L. Tan, T. Friis, C. Wu, R. Crawford, Y. Xiao, Osteoimmunomodulatory properties of magnesium scaffolds coated with beta-tricalcium phosphate, Biomaterials, 35 (2014) 8553-8565.

[46] T. Fernandes, J. Hodge, P. Singh, D. Eeles, F. Collier, I. Holten, P. Ebeling, G. Nicholson, J. Quinn, Cord Blood-Derived Macrophage-Lineage Cells Rapidly Stimulate Osteoblastic Maturation in Mesenchymal Stem Cells in a Glycoprotein-130 Dependent Manner, PloS one, 8 (2013) e73266.